Cooperative Subunit Interactions in C-Type Inactivation of K Channels

E. M. Ogielska, W. N. Zagotta, T. Hoshi, S. H. Heinemann, J. Haab, and R. W. Aldrich
Howard Hughes Medical Institute and Department of Molecular and Cellular Physiology, Stanford University School of Medicine, Stanford, California 94305 USA

ABSTRACT C-type inactivation of potassium channels is distinct from N-terminal mediated (N-type) inactivation and involves a closing of the outer mouth of the channel. We have investigated the role of the individual subunits of the tetrameric channel in the C-type inactivation conformational change by comparing the inactivation rates of channels constructed from different combinations of subunits. The relationship between the inactivation rate and the number of fast subunits is exponential, as would be predicted by a cooperative mechanism where the C-type conformational change involves all four subunits, and rules out a mechanism where a conformational change in any of the individual subunits is sufficient for inactivation. Subunit interactions in C-type inactivation are further supported by an interaction between separate mutations affecting C-type inactivation when in either the same or separate subunits.

INTRODUCTION

Most voltage-gated ion channels undergo inactivation after opening. The inactivation process is important for the generation and integration of electrical signals and can occur over a wide range of time courses in different types of channels. An individual channel molecule can have multiple distinct types of inactivation occurring over different time courses (Hodgkin and Huxley, 1952; Narahashi, 1974; Adelman and Palti, 1969; Chandler and Meves, 1970; Khodorov et al., 1976; Ehrenstein and Gilbert, 1966; Hoshi et al., 1991; Choi et al., 1991). The molecular mechanisms of two distinct types of inactivation of voltage-gated potassium channels, N-type and C-type, have been investigated. N-type inactivation is better understood and has been shown to occur through a "ball-and-chain" mechanism (Hoshi et al., 1990; Zagotta et al., 1990) originally proposed for Na^+ channel inactivation (Armstrong and Bezanilla, 1977). An N-terminal domain binds to the internal mouth of the channel, occluding the ion permeation pathway (Hoshi et al., 1990; Zagotta et al., 1990; Demo and Yellen, 1991). N-type inactivation is voltage independent, is coupled to activation, and is complete within 2–3 ms in *Shaker* B (*Sh*B) channels. C-type inactivation occurs much more slowly in *Sh*B channels but can be quite fast in other alternatively spliced *Shaker* channel variants (Hoshi et al., 1991; Iverson and Rudy, 1990). Like N-type inactivation, C-type inactivation is coupled to activation and is voltage independent between −25 mV and +50 mV. Although C-type inactivation may be studied in the absence of N-type inactivation, it is in fact partially coupled to N-type inactivation and occurs faster from the N-type inactivated state (Hoshi et al., 1991; Baukrowitz and Yellen, 1995).

In Shaker channels with the amino-terminal region removed to eliminate N-terminal inactivation, substitution of residues in the sixth membrane-spanning region (S6) and the P-region have been shown to affect the time course of C-type inactivation (Hoshi et al., 1991; Labarca and MacKinnon, 1992; Heginbotham et al., 1994; DeBiasi et al., 1993). A single amino acid difference (alanine to valine) at position 463 in S6 is responsible for the approximately 100-fold difference in C-type inactivation rate between two alternatively spliced variants (Hoshi et al., 1991). Amino acid substitutions in the P-region at position 449, a threonine in the wild-type *Sh*B channel, can also alter the C-type inactivation rate by several orders of magnitude (Lòpez-Barneo et al., 1993).

Although the molecular mechanism of C-type inactivation is not understood, several lines of evidence favor the hypothesis that inactivation occurs through a constriction of the outer mouth of the pore. Application of external tetraethylammonium (TEA), a pore blocker, competes with C-type inactivation but has no effect on N-type inactivation (Choi et al., 1991). Slowing of C-type inactivation has also been observed in experiments where the concentration of external K^+ or Rb^+ has been elevated (Lòpez-Barneo et al., 1993; Labarca and MacKinnon, 1992; Baukrowitz and Yellen, 1995). Both of these results are consistent with a "foot-in-the-door" mechanism where the presence of external TEA or a permeant ion prevents the closing of the outer mouth of the channel protein. There is additional evidence suggesting that C-type inactivation is accompanied by a structural rearrangement of the external mouth of the pore near position 449. The introduction of a cysteine at 449

Received for publication 26 July 1995 and in final form 6 September 1995.

Address reprint requests to Dr. R. W. Aldrich, Department of Molecular and Cell Physiology, Stanford University School of Medicine, HHMI-Beckman Center, Stanford, CA 94305-5426. Tel.: 415-723-6531; Fax: 415-725-4463; E-mail: raldrich@leland.stanford.edu.

The present address of Dr. Zagotta is Department of Physiology and Biophysics, SJ-40, University of Washington, Seattle, WA 98915.

The present address of Dr. Hoshi is Department of Physiology and Biophysics, University of Iowa, Iowa City, IA 52242-1109.

The present address of Dr. Heinemann is Max-Planck-Gesellschaft z.F.d.W. AG Molekulare und zelluläre Biophysik, Drackendorfer Strasse 1, D-07747 Jena, Germany.

The present address of Dr. Haab is Institute of Neuroscience, University of Oregon, Eugene, OR 97403.

0006-3495/95/12/2449/09 $2.00

renders the channel sensitive to block by cadmium (Yellen et al., 1994). Cadmium blocking experiments suggest that the C-type inactivated state is much more sensitive to cadmium than either the open or the closed state (Yellen et al., 1994). The state dependence of the block suggests either a physical rearrangement during the C-type inactivation process where residue 449 becomes exposed to solution in the inactivated state, or the spatial distribution of the cysteines changes, creating a more efficient binding site for cadmium.

In this study, we examine the interactions between subunits during the C-type inactivation conformational change and the interactions between mutations at position 463 in S6 and position 449 in the P-region. We address two specific questions: 1) Do the changes of inactivation rates with mutations of residues 449 and 463 affect the same or different inactivation processes? 2) Is a conformational change in one subunit sufficient for C-type inactivation to occur, or does it occur by a concerted conformational change? A preliminary report of this work has been presented in abstract form (Ogielska et al., 1994).

MATERIALS AND METHODS

Molecular biology

The *Sh*BΔ6-46 deletion that removes N-type inactivation was generated as described previously (Hoshi et al., 1990). Point mutations at positions T449 and A463 were made by generating PCR primers using *Sh*BΔ6-46 as the template. The PCR product was gel purified and spliced into either the A protomer or the B protomer using *Nsi*I and *Hind*III as the restriction sites (Hoshi et al., 1991; Lòpez-Barneo et al., 1993). The A protomer contains a nine-amino acid linker at the end of the C-terminus (NNNNNNAMV), which allows the two protomers to be ligated after an *Nco*I and *Kpn*I digestion of both protomers (Heginbotham and MacKinnon, 1992). To check that the proper monomers were linked together and that no secondary mutations occurred, the dimers were separated using *Nco*I, and the mutated region of each monomer subunit was sequenced after the fragment was gel purified. The resultant dimers were linearized using either *EcoR*I or *Kpn*I, and RNA was synthesized using the T7 RNA polymerase from the Message Machine kit from Ambion. The $A_{463V}B$ dimer was made two separate times, but neither time did this construct lead to expressed potassium channels in oocytes.

Electrophysiology and analysis

The transcribed RNA was injected into *Xenopus laevis* oocytes as previously described (Zagotta et al., 1989). Macroscopic and single-channel recordings were done in cell-free patches 3–10 days post-injection. Macroscopic currents were recorded using pipettes with initial resistances of <2 MΩ, and no corrections were made for series resistance. Leak subtraction was done using the P/4 protocol. All recordings were done at 21°C. The internal solution contained (in mM): 140 KCl, 2 $MgCl_2$, 10 EGTA, and 10 HEPES at a pH of 7.2. The external solution contained (in mM): 140 NaCl, 4 $MgCl_2$, 2 $CaCl_2$, 2 KCl, and 5 HEPES at a pH of 7.1. The TEA blocking experiments were done in the outside-out configuration, where 140 mM TEACl solution was mixed with the 140 mM NaCl solution at the appropriate volumes to achieve the desired concentrations.

The AB_{T449K} heterotetramer expressed very poorly, and consequently the majority of the data were from single-channel patches. The ensemble averages of the single-channel records as well as the macroscopic data were fitted with single exponentials to obtain the time constant of C-type inactivation. A fast initial component of inactivation was observed in some patches but was ignored for the fit. The wild-type C-type inactivation time course typically did not fall to zero during the 7600-ms pulse. The calculations of rate constants were therefore corrected for recovery. $(a - b)/a = k/(k + k_{-1})$, where a is the peak current amplitude, b is the steady-state component of the current, and k and k_{-1} are the forward and reverse rate constants, respectively.

RESULTS

Previous studies have shown that substitutions at positions T449 (in the P region) or A463 (in S6) in the *Sh*B variant with N-type inactivation removed (*Sh*BΔ6-46) cause significant changes in the rate of C-type inactivation (Hoshi et al., 1991; Lòpez-Barneo et al., 1993). Fig. 1 shows the effects of these single substitutions as well as the effects of mutating both positions simultaneously. The amino acid at position 449 is listed vertically and the amino acid at position 463 is listed horizontally. As previously described, the rate of C-type inactivation is sensitive to the residue at position 449: fast inactivation in channels with a glutamic acid, lysine, or alanine; slower inactivation with a threonine (wild type) or histidine; and very slow inactivation with either a tyrosine or valine. Substitution of alanine at position 463 to a valine in the wild-type channel increases the inactivation rate 100-fold (Hoshi et al., 1991).

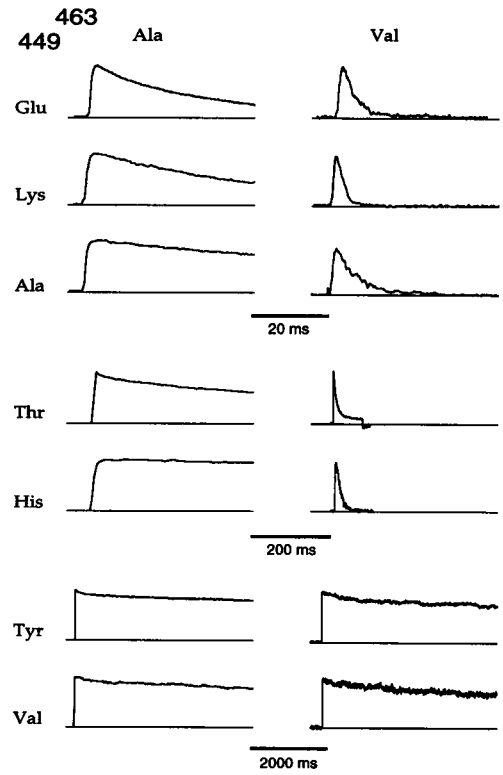

FIGURE 1 Effects of single and double mutations at positions T449 and A463. Representative currents from constructs containing a mutation at position 449 (*vertical*) and/or position 463 (*horizontal*). The amino acid substitution is denoted by a three-letter code. The wild-type *Sh*B channel contains a threonine at position 449 and an alanine at position 463. Currents were elicited by steps to +50 mV from holding potentials between −80 mV and −120 mV. Current amplitudes were scaled for comparison purposes; note the different time scales.

If mutations at position 449 and position 463 altered the rates of separate inactivation processes, channels with a valine at position 463 would inactivate quickly, regardless of the amino acid at position 449. If position 449 is occupied by a glutamic acid, lysine, alanine, threonine, or histidine, an additional substitution from wild-type alanine to a valine at position 463 causes a substantial increase of the inactivation rate. However, when occupied by either tyrosine or valine, position 449 appears to play a dominant role in determining the overall inactivation rate, regardless of whether a valine or alanine is at position 463. This interaction of mutations at the two positions demonstrates that they are affecting the same or strongly coupled processes of inactivation (C-type) rather than independent (C-type and previously undescribed) inactivation processes.

One interpretation of this result is that the mutations are not energy additive and are interacting with one another either directly or indirectly. An alternative interpretation is that the mutations are energetically additive, but the equilibrium between the noninactivated and the inactivated state in the 449Y mutant is so heavily biased toward the open state that the additional 463V mutation is not able to noticeably affect that equilibrium.

Functional stoichiometry of C-type inactivation

We took advantage of the effects of amino acid substitutions on the inactivation rate and the tetrameric structure of the *Shaker* channel (MacKinnon, 1991; Liman et al., 1992) to explore the functional stoichiometry of C-type inactivation. It is possible that a conformational change in a single subunit could be sufficient to cause C-type inactivation to occur. Alternatively, all four subunits may undergo highly cooperative or concerted conformational transitions. To differentiate between these possibilities, we made use of the expression of tandem dimer constructs where two α subunit cDNAs are linked (Isacoff et al., 1990; Heginbotham and MacKinnon, 1992). We constructed tandem dimers with one subunit containing a mutation that increased the inactivation rate of the channel and one wild-type (slowly inactivating) subunit. The heteromultimeric channels, arising from the assembly of two tandem dimers into a tetrameric channel, are predicted to have different inactivation rates, depending on whether the fast and slow subunits interact in a cooperative mechanism, or whether an independent conformational change in any one of the subunits is sufficient to cause inactivation.

If the mechanism is independent, where a conformational change in a single subunit is sufficient to inactivate the channel, then the inactivation rate constant will be the sum of the individual rate constants contributed by each of the four subunits:

$$k = \sum k_{\text{subunit}}. \tag{1}$$

For a heterotetrameric channel with a combination of n fast and $4 - n$ slow subunits:

$$k = \frac{nk_{\text{fast}}}{4} + \frac{(4-n)k_{\text{slow}}}{4}, \tag{2}$$

where k_{fast} and k_{slow} are the inactivation rates of the fast and slow homomultimers, respectively. For the case of channels formed from two dimers, each with one fast and one slow subunit,

$$k = \frac{(k_{\text{fast}} + k_{\text{slow}})}{2}. \tag{3}$$

If the process of C-type inactivation is concerted (highly cooperative), involving a conformational change in the channel tetramer, then each of the four subunits of the channel will contribute free energy to the transition state for the inactivation conformational change, and the inactivation rate for a channel with a combination of n fast and $4 - n$ slow subunits will be exponentially related to the sum of the energetic contributions of the individual subunits:

$$k = A \exp \frac{-(n\Delta G_1^{\ddagger} + (4-n)\Delta G_2^{\ddagger})}{k_B T}, \tag{4}$$

where A is the attempt frequency (10^{12} s^{-1}),

$$\Delta G_1^{\ddagger} = \frac{\left(-k_B T \ln\left(\frac{k_{\text{fast}}}{A}\right)\right)}{4},$$

and

$$\Delta G_2^{\ddagger} = \frac{\left(-k_B T \ln\left(\frac{k_{\text{slow}}}{A}\right)\right)}{4}.$$

For a channel with two slow and two fast subunits the predicted inactivation rate for a concerted mechanism would be

$$k = A \exp \frac{-2(\Delta G_1^{\ddagger} + \Delta G_2^{\ddagger})}{k_B T}. \tag{5}$$

The off rates may be ignored if the current decays to zero at long times. In this case the channel's recovery from inactivation is so slow that its contribution to the measured current is not appreciable. This was true for the 449K and 463V mutant channels. However, even at positive potentials the off rate is small but appreciable in wild-type channels, as is evident from the small steady-state current in the set of traces in Fig. 2 *B*. For our analysis the inactivation rates of wild-type channels are calculated from exponential fits to the current decay and the steady-state current as described in Materials and Methods.

To engineer hybrid channels with two fast and two slow subunits, we linked the cDNA of two subunits, in a single open-reading frame, separated by a short oligonucleotide linker (a gift of Rod MacKinnon) (Isacoff et al., 1990; Heginbotham and MacKinnon, 1992). The mutations were made in this dimer background. Such dimer constructs have

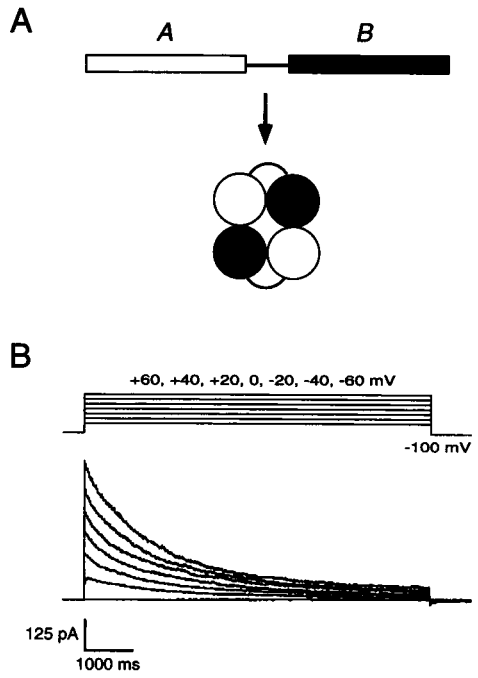

FIGURE 2 Formation of tetrameric channels from dimers. (*A*) Cartoon predicting channel formation from concatenated dimer subunits. The dimer constructs may contain a mutation in either the first or second subunit (see Experimental Procedures). (*B*) Representative traces from tandem-linked wild-type *Sh*BΔ6-46 channels. Macroscopic currents were recorded in an outside-out patch in response to 7600-ms voltage pulses ranging from −60 mV to +60 mV in 20-mV increments from a holding potential of −100 mV every 22 s.

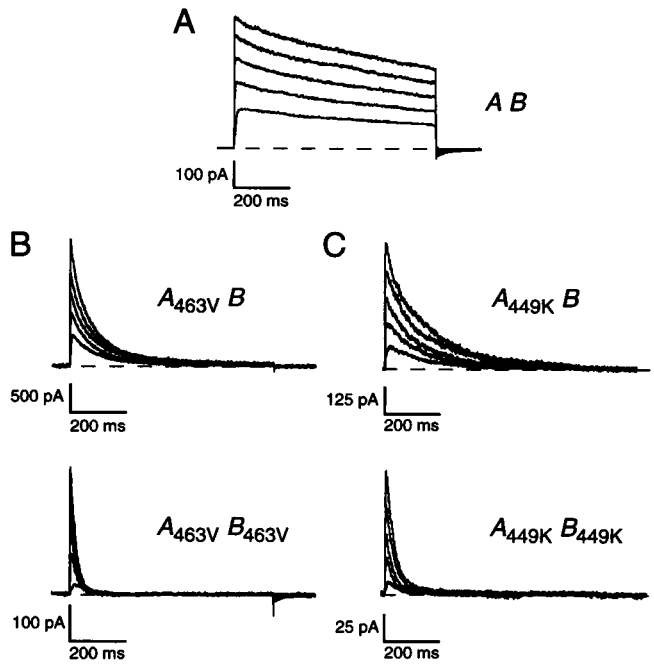

FIGURE 3 Current families for homomultimers and heteromultimers containing mutations at either position A463 or T449. (*A*) Comparison of traces from tandem-linked wild-type *Sh*BΔ6-46 channels. Steps are from a holding potential of −100 mV to voltages between −40 mV and 40 mV in 20 mV increments for a duration of 760 ms. The interpulse interval was 10 s. (*B*) Traces from constructs containing a mutation at position 463 from an alanine to a valine. The top set of traces is from channels with the A463V mutation in two of the four subunits, and the bottom set contains the A463V mutation in all four subunits. Pulse protocol as in *A*. (*C*) Traces from constructs containing a mutation at position 449 from a threonine to a lysine. The top set of traces contains the T449K mutation in two of the four subunits, and the bottom set contains the T449K mutation in all four subunits. Pulse protocol as in *A*, but from a holding potential of −80 mV.

been shown to form tetrameric channels as shown in Fig. 2 *A*, although missassembly may occur (see below). The mutation may be made in either the first or the second subunit of the dimer. If the dimeric constructs assemble correctly as shown in Fig. 2 *A* and if the linker does not affect the inactivation process, they should have the same properties regardless of whether the mutation was made in the first or second subunit. Although a subset of the formed channels may be missassembled, this approach has been shown to be quite successful if the appropriate controls are done (Isacoff et al., 1990; Heginbotham and MacKinnon, 1992; McCormack et al., 1992). Channels formed from wild-type *Sh*BΔ6-46 dimers behave as would be predicted from the behavior of wild-type *Sh*BΔ6-46 channels formed from monomer subunits (see Figs. 2 *B* and 3 *A*).

In the first set of experiments the alanine at position 463 in S6 was mutated to a valine in either one or both of the dimer subunits. The mutation speeds the time constant of inactivation roughly 100-fold (~1500 ms to ~15 ms) in homotetramers. The off rate is extremely slow, with less then 25% of the inactivated channels returning from inactivation after 1 s at −100 mV (Hoshi et al., 1991). Representative traces from the A463V homomultimer assembled from tandem dimers are shown at the bottom of Fig. 3 *B*. The top set of traces in Fig. 3 *B* is from channels where only one subunit was mutated in the dimer construct. The heteromultimeric channel is presumed to have two slow (wild-type) and two fast (A463V) subunits.

In the second set of experiments the mutation is made at position 449 with the threonine replaced with a lysine. This single substitution speeds up the time constant of inactivation from ~1500 ms to ~25 ms in homotetramers. The recovery rate is similar to that of wild-type channels. Representative traces for the T449K homomultimer assembled from tandem dimers are shown in the bottom of Fig. 3 *C*, where both halves of the dimer carry the T449K mutation. The top family of traces in Fig. 3 *C* is from the heteromultimeric channel containing two slow (wild-type) and two fast (T449K) subunits. The wild-type, A463V, and T449K homotetrameric channels made from tandem dimers inactivate with rates similar to the respective homotetrameric channels assembled from monomers, consistent with correct assembly of the tetramers.

The comparison of both sets of data to the theoretical predictions of the independent and concerted mechanisms is shown in Fig. 4, *A* and *B*. For the heteromultimers ($A_{449K}B$, AB_{449K}, $A_{463V}B$) the current traces decayed to zero, therefore the inactivation return rates were insignificant. The

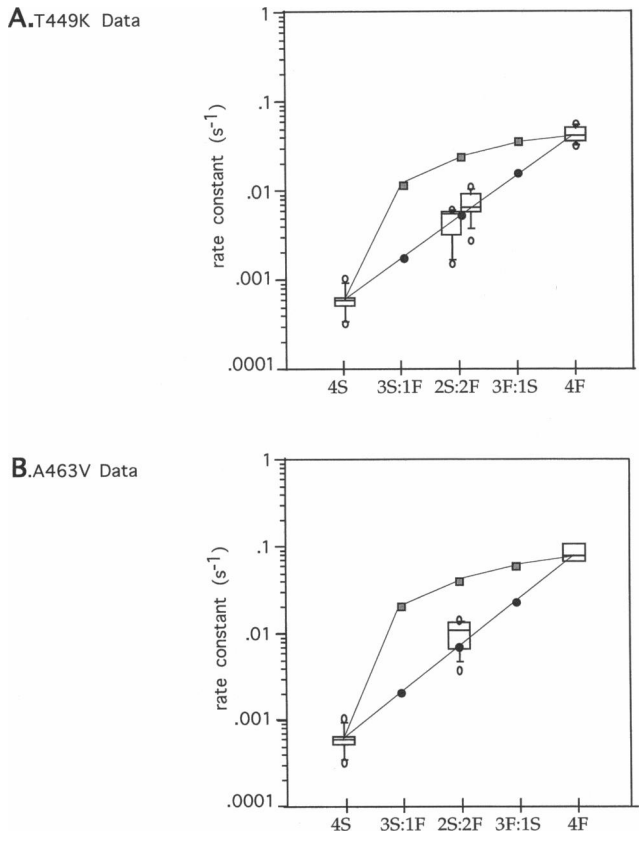

FIGURE 4 Box plots of the rates of C-type inactivation for constructs with either the mutation T449K (*A*) or A463V (*B*). Macroscopic currents were fitted with single exponentials using the least-squares method. Wild-type currents were corrected for a nonzero steady-state current (see Materials and Methods). The time constants were converted to rate constants ($\tau = 1/k$). The rate constants are shown on the *y* axis on a logarithmic scale. The central outlined box shows the middle half of the data, between approximately the 25th and the 75th percentiles. The horizontal line within the box represents the median of the data. The "whiskers" reflect the main body of the data, and the separately plotted points show the outliers (Tukey, 1977). Sample sizes were between 6 and 13 (*A*) and 3 and 13 (*B*). The *x* axis shows the stoichiometry of the constructs in terms of the number of fast and slow subunits. In *A* there are two box plots for 2S:2F because the mutation was made in either the first or the second half of the dimer. In *B* only the mutant with the A463V mutation in the first half of the dimer expressed. The dark circles represent the predicted rates from the fully cooperative mechanism (Eq. 4), and the dark squares represent the predicted rates if the mechanism of C-type inactivation was independent (Eq. 2).

records were fitted with single exponentials and the resultant rate constants from many patches are plotted as box plots on the *y* axis. The *x* axis denotes the number of slow and fast subunits in each channel type. The predictions are shown as filled circles for the concerted case and filled squares for the independent case. Predictions were calculated as explained earlier for all five possible combinations of fast and slow subunits. For the T449K mutations, data are shown for constructs with the mutation in either the first or second half of the dimer (Fig. 4 *A*). The similarity in the distributions of rate constants indicates that the subunits formed correctly for the most part, although there is a slight but insignificant tendency for faster inactivation when the 449K mutation is in the first subunit of the dimer. For the 463 mutation, the dimers with the reverse orientation did not express in oocytes. The data for both the A463V and T449K mutations fit the concerted model rather than the independent one.

Intersubunit interactions

We have shown that the C-type inactivation mechanism involves cooperative interactions between the four subunits and that the mutations at positions 449 (in the P-region) and 463 (in S6) do not affect C-type inactivation independently. Specifically, if position 449 is occupied by either a valine or a tyrosine an additional substitution to a valine at position 463 has no further effect on the C-type inactivation rate. These results raise an interesting question about intersubunit interactions: If the two mutations are placed in separate subunits of the channel, will this dominant effect of residues at position 449 over position 463 be preserved across subunits?

To investigate the possibility of intersubunit interactions between mutations at positions 449 and 463 we again utilized dimeric channel constructs. Two sets of dimers were compared. One construct (test) contained a T449Y mutation in one dimer subunit and a A463V mutation in the other dimer subunit. Assuming correct assembly (see below), the resultant channel contained two subunits with tyrosines at position 449 (slow) and wild-type alanines at position 463 (449Y: 463A), and two subunits with wild-type threonines at position 449 and valines (fast) at position 463 (449T: 463V). The second construct (control) is made up of one subunit with both substitutions, T449Y and A463V, and one wild-type subunit. The resultant channels, if correctly assembled, would have two 449Y:463V subunits and two wild-type (449T:463A) subunits. Thus, there is no difference in amino acid substitutions between the test construct and the control except for the subunit in which they were placed.

The question is whether the tyrosine at position 449 can dominate the effect of the valine at position 463 in another subunit (as it does when both mutations are in the same subunit) and slow down the overall inactivation rate of the channel. If the dominant effect cannot be transferred across subunits, the test channel should have a relatively fast time constant, as predicted by the cooperative mechanism (Eq. 5) for two slow and two fast subunits, assuming no extra interactions.

The T449Y mutant does not inactivate during a 10-s pulse, making it difficult to obtain an accurate measurement of the time constant. The three predictions were calculated, each assuming a different plausible (slow) inactivation time constant for the T449Y mutant. The values of 10,000 ms, 30,000 ms, and 100,000 ms were used as approximations for the T449Y mutant, and 15 ms is the empirically determined inactivation time constant for A463V. The predictions are

382 ms, 674 ms, and 1248 ms, respectively, depending on the value used for the inactivation time constant of T449Y. The predicted time constant of inactivation for the heteromultimers only increases roughly threefold for a 100-fold increase in the inactivation time constant of the T449Y mutant. If the dominance is preserved across subunits, then the inactivation rate of the test channels would be considerably slower than these predicted rates. The control heteromultimer is also expected to display a slow inactivation rate, as predicted by the concerted mechanism (Eq. 5) for two slowly inactivating subunits.

Currents from the test and control channels are shown in Fig. 5 *A*. The top trace shows the current elicited by a 7600-ms step to +50 mV for the control construct. The inactivation rate is slow, as expected for a channel with four slowly inactivating subunits. The current from the test construct is shown in the bottom trace of Fig. 5 *A*. It does not fully inactivate during the 7600-ms pulse. The three predicted traces, assuming no intersubunit interactions between the tyrosine at position 449 in one subunit and the valine at position 463 in another subunit, are shown superimposed as dashed lines. The channels inactivate with a time course similar to the control channels and much slower than the predictions, which assumed no intersubunit interactions between 449 and 463, even if the 449Y time constant is as slow as 100 s. The slow inactivation time course is a reproducible feature of the $A_{463V}B_{449Y}$ construct (n = 5).

We have taken the very slow and slight current decay in 449Y channels to reflect an extremely slow inactivation rate or a noninactivating channel (Lòpez-Barneo et al., 1993). This assumption is supported by the observation that 449Y current continues to decay during pulses up to 50 s in duration (Lòpez-Barneo et al., 1993; E. Ogielska, unpublished observation). However, there is some uncertainty in attributing all of the decay to C-type inactivation as opposed to some other, slower form of inactivation during such long pulses. In this interpretation, the high current level observed at the end of the 7.6-s pulse in the $A_{463V}B_{449Y}$ construct (Fig. 5 *A*) results from an extremely slow inactivation, and not from a rapid but incomplete inactivation. The high steady-state component could be due to fast recovery if 449Y inactivated quickly and recovered quickly. If this were the case then we would expect the 449Y current traces to show a very fast initial component and a high steady-state component. A fast initial component is sometimes observed; however, it is not reliably reproducible and it has also been observed in wild-type currents, which inactivate slowly. It is therefore our conclusion that the dominant effects of a tyrosine at position 449 can in fact be extended across subunits.

This conclusion depends on the assumption of correct assembly of the tetrameric channels from the tandem dimers. Previous work has shown that such dimers do not always assemble properly (McCormack et al., 1992). Sometimes the first half of the dimer is preferentially incorporated, creating channels with different stoichiometries than were originally intended. One way to control for this problem is to express both possible constructs, one with the mutation in the first subunit of the dimer and the other with the mutation in the second subunit. These should give similar results if the dimers are assembling correctly into tetrameric channels. This prediction has been borne out in the case of the $A_{449K}B$ and AB_{449K} heteromultimers. As seen in Fig. 4 *A*, the $A_{449K}B$ construct, with the mutation that confers fast inactivation in the first half, appears to have given rise to a small population of channels with preferentially incorporated A_{449K} subunits, because the overall inactivation rate is slightly faster than that of channels made up of dimers wth the mutation in the second half. Although

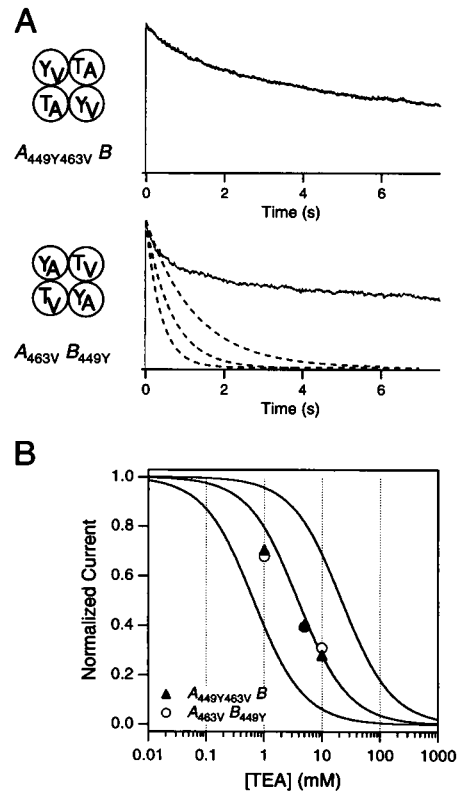

FIGURE 5 (*A*) A representative trace from a heteromultimer containing an A463V mutation and a T449Y mutation in two subunits and two wild-type *Sh*BΔ6-46 subunits (control) (*top*) and a representative trace from a heteromultimer containing the A463V mutation in two subunits and the T449Y mutation in the other two subunits (*test*) (*bottom*). In both cases the data were taken from outside-out patches. Current was elicited by 7600-ms steps to +50 mV from a holding potential of −80 mV. The dashed curves, superimposed on the test trace, on the bottom of *A* represent the predictions for the inactivation time constant of that particular construct, given full cooperativity among the four subunits and assuming no extra interactions (see text for details). (*B*) Test of proper assembly using external TEA. The solid curves show the predicted TEA sensitivities based on energy additivity studies (Heginbotham and MacKinnon, 1992). The rightmost curve predicts the sensitivity of wild-type *Shaker* channels, the middle curve shows the predictions for the case where two 449 residues contain threonines and two contain tyrosines, and the leftmost curve predicts the behavior of channels with four tyrosines at position 449. The circles represent the TEA sensitivity of the patch shown in the top half of *A* ($A_{449Y463V}B$), and the triangles show the TEA sensitivity of the patch shown in the bottom of *B* ($A_{463V}B_{449Y}$).

the preferential incorporation of the first half of the dimer is reflected in the inactivation rates of the constructs, these differences are not significant, confirming proper assembly of the majority of the channels.

With the mutations employed in the present experiments, correct assembly can also be assessed by testing the channel's sensitivity to external TEA. Replacing the wild-type threonine at position 449 in *Shaker* with a tyrosine greatly enhances TEA sensitivity, and channels assembled from dimers containing two tyrosines and two threonines have intermediate TEA sensitivity (Heginbotham and MacKinnon, 1992; Kavanaugh et al., 1992). Fig. 5 *B* shows the TEA sensitivity of the test and control traces shown in Fig. 5 *A*. The solid curves show the predicted TEA binding curves for channels with four tyrosines at 449 (*leftmost curve*), two tyrosines and two threonines (*middle curve*), and four threonines (*rightmost curve*) (from Heginbotham and MacKinnon, 1992). The TEA sensitivity was tested on the same patch that the inactivation time constant was measured from. The data show the TEA sensitivity as expected for correctly assembled subunits, with two threonines and two tyrosines at position 449.

Fig. 6 *A* shows the TEA sensitivity of all the other patches with channels assembled from the $A_{449Y}B_{463V}$ dimer as well as the converse mutation $A_{463V}B_{449Y}$. The channels formed from the $A_{463V}B_{449Y}$ dimers formed correctly, as shown in Fig. 6 *A* (*filled symbols*). However, the channels formed from the $A_{449Y}B_{463V}$ dimers did not assemble correctly (Fig. 6 *A*, *open symbols*). It appears that the first subunits of the dimer preferentially assembled, giving rise to channels composed mainly of subunits with the T449Y mutation and therefore a greater sensitivity to TEA. The molecular basis for the missassembly of this one set of constructs is not understood. Because of misassembly we cannot interpret the results obtained with this construct. The fact that one of our test constructs ($A_{449Y}B_{463V}$) did not assemble as predicted does not invalidate our conclusions. The TEA experiments show that the converse test construct, $A_{463V}B_{449Y}$, did assemble properly, and as a result we are confident in our interpretation of the data (see Fig. 5). Fig. 6 *B* shows the TEA sensitivity of the control heteromultimers, $A_{449Y463V}B$ and $AB_{449Y463V}$. The data show the TEA sensitivity as expected for correctly assembled subunits.

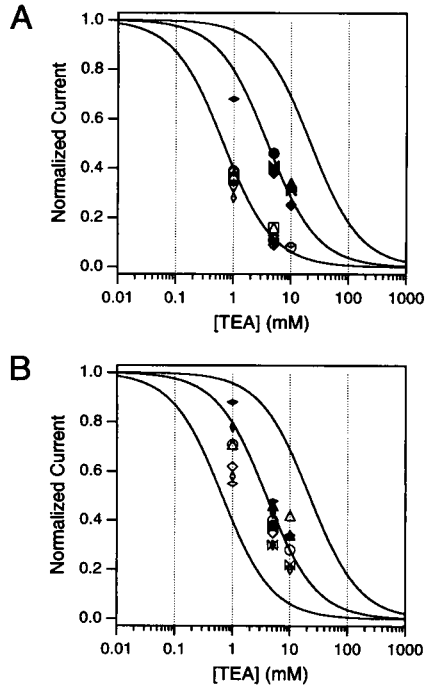

FIGURE 6 TEA sensitivity of the heteromultimeric channels. The TEA sensitivities of all of the intersubunit interaction heteromultimers were tested, and the outcomes are plotted as described in Fig. 5 *B*. The top panel shows the TEA sensitivities of the $A_{463V}B_{449Y}$ construct (*filled symbols*) and the converse $A_{449Y}B_{463V}$ construct (*open symbols*). The bottom panel shows the TEA sensitivities of the $A_{449Y463V}B$ construct (*open symbols*) and the converse $AB_{449Y463V}$ construct (*filled symbols*). In all cases the different symbol types represent data from different outside-out patches.

DISCUSSION

We have utilized different mutations at position 449 in the outer mouth of the pore and position 463 in S6 to examine the nature of subunit interactions during the process of C-type inactivation. We have presented two lines of evidence for a concerted or cooperative conformational change in C-type inactivation: 1) The overall inactivation rate is exponentially related to the sum of the individual transition state free energies contributed by each of the four subunits (rather than a sum of the rates). 2) Mutations at residues 449 and 463 interact, even when in different subunits.

The interaction between certain mutations at positions 449 and 463 suggest that alterations of the two residues affect the same process of inactivation. Our results do not rule out the possibility that the mutations at positions 449 and 463 affect different but highly coupled inactivation processes or the possibility of other inactivation mechanisms in addition to N-type and C-type. The possibility of there being different inactivation mechanisms is not necessarily unreasonable because *Shaker* channels without an N-type inactivation domain can inactivate with a multiexponential time course. In some cases our data could be better fitted with a decay described by the sum of two exponentials. The data, however, were usually approximated well by a single exponential decay.

We took advantage of the effects of mutations at T449 and A463 on the inactivation rate to determine the stoichiometry of the C-type inactivation process. Our data indicate that the inactivation rate of the heteromultimers can be explained by transition state energy additivity (Eqs. 4 and 5) among subunits and therefore that C-type inactivation involves a cooperative conformational change. Our data are inconsistent with a fully independent mechanism of inactivation and with a model where each subunit undergoes the open to inactivated transition independently but requires all four subunits to make the transition before the channel is inactivated. The latter model would predict that the hetero-

multimeric channels would inactivate with a time course equal to or slower than that of the slowest subunit, which our data definitely exclude. It is not possible from our analysis to determine the strength of the cooperative interactions between subunits or the mechanisms of cooperative subunit interactions. However, the data agree well with the predictions of a fully cooperative model. It is also important to note that the process appears cooperative regardless of whether the fast substitution was made at position 449 or 463, supporting the argument that both mutations are affecting the same inactivation process. The cooperativity observed here is consistent with results from cadmium blocking experiments which suggested that the spatial distribution of each of the four residues at position 449 changes during the process of C-type inactivation, rendering the channel more capable of coordinating the cadmium ion (Yellen et al., 1994). A cooperative mechanism for C-type inactivation in a related potassium channel, $K_V1.3$, has also been reported (Panyi et al., 1995). A concerted C-type conformational change differs from the mechanism of N-type inactivation, where amino-terminal blocking domains on each of the subunits function independently (MacKinnon et al., 1993).

Somewhat surprisingly, we found that the dominance of 499Y over 463V could be transferred across subunits. It seems unusual that the dominant effect of one mutation over another is preserved regardless of whether the two are placed in the same or different subunits. The apparent paradox could be resolved if both the intrasubunit and intersubunit interactions are mediated through the ion-conducting pore rather than through direct side chain or backbone interactions. Perhaps the mutations are affecting inactivation indirectly through effects on ion occupancy in the channel. The C-type inactivation rate is quite sensitive to permeant ions, and that sensitivity can be altered by mutations in the pore and in S6 (Lòpez-Barneo et al., 1993, Labarca and MacKinnon, 1992; Baukrowitz and Yellen, 1995; E. Ogielska and P. Zei, unpublished observations). If both residues 449 and 463 affect the probability of ion occupancy in the pore either directly, by extending into part of the ion conducting pathway, or indirectly, perhaps by backbone structural alterations, then their effect could be the same, regardless of whether the mutations were made in the same or different subunits, assuming each subunit contributes equally to the pore. Although this hypothesis requires further testing, several lines of evidence are consistent. Position 449 has been localized at the external mouth of the pore (Heginbotham and MacKinnon, 1992; Lu and Miller, 1995; Kurz et al., 1995). At least part of S6 has been implicated as lining part of the pore (Choi et al., 1992; Lopez et al., 1994). The alanine to valine change at 463 in S6 changes the single-channel conductance by about twofold in physiological solutions (Hoshi et al., 1991 and unpublished data), consistent with at least an indirect effect of this position on ion permeation. Mutations of other pore-lining residues interact when in the same or different subunits (Kirsch et al., 1992, 1993). Mutations at other putative pore-lining residues affect C-type inactivation (Labarca and MacKinnon, 1992; DeBiasi et al., 1993; Heginbotham et al., 1994). Understanding of the mechanism of interactions between subunits in C-type inactivation would benefit from a more detailed examination of the intra- and intersubunit interactions of other residues in and around the pore.

We thank R. MacKinnon for the kind gift of the A and B protomers and E. Hazel for help with analysis.

This work was supported by a grant from the National Institutes of Health (NS23294), a National Institutes of Health training grant (GM08327) to E. M. Ogielska, and a National Institute of Mental Health Silvio Conte Center for Neuroscience Research grant (MH 48108). R. W. Aldrich is an investigator with the Howard Hughes Medical Institute.

REFERENCES

Adelman, W. J., Jr., and Y. Palti. 1969. The effects of external potassium and long duration voltage conditioning on the amplitude of sodium currents in the giant axon of the squid, *Loligo paelei*. *J. Gen. Physiol.* 54:589–606.

Armstrong, C. M., and F. Bezanilla. 1977. Inactivation of the sodium channel. II. Gating current experiments. *J. Gen. Physiol.* 70:567–590.

Baukrowitz, T., and G. Yellen. 1995. Modulation of K current by frequency and external $[K^+]$: a tale of two inactivation mechanisms. *Neuron.* In press.

Chandler, W. K., and H. Meves. 1970. Slow changes in membrane permeability and long-lasting action potentials in axons perfused with fluoride solutions. *J. Physiol.* 211:707–728.

Choi, K. L., R. W. Aldrich, and G. Yellen. 1991. Tetraethylammonium blockade distinguishes two inactivation mechanisms in voltage-activated K channels. *Proc. Natl. Acad. Sci. USA.* 88:5092–5095.

Choi, K. L., C. Mossman, J. Aube, and G. Yellen. 1992. The internal quaternary ammonium receptor site of *Shaker* potassium channels. *Neuron.* 10:533–541.

DeBiasi, M., H. A. Hartmann, J. A. Drewe, M. Taglialatela, A. M. Brown, and G. E. Kirsch. 1993. Inactivation determined by a single site in K^+ pores. *Pflügers Arch.* 422:354–363.

Demo, S. D., and G. Yellen. 1991. The inactivation gate of the Shaker K^+ channel behaves like an open channel blocker. *Neuron.* 7:743–753.

Ehrenstein, G., and D. L. Gilbert. 1966. Slow changes of potassium permeability in the squid giant axon. *Biophys. J.* 6:553–566.

Heginbotham, L., Z. Lu, T. Abramson, and R. MacKinnon. 1994. Mutations in the K^+ channel signature sequence. *Biophys. J.* 66:1061–1067.

Heginbotham, L., and R. MacKinnon. 1992. The aromatic binding site for tetraethylammonium ion on potassium channels. *Neuron.* 8:483–491.

Hodgkin, A. L., and A. F. Huxley. 1952. The dual effect of membrane potential on sodium conductance in the giant axon of *Loligo*. *J. Physiol.* 116:497–506.

Hoshi, T., W. N. Zagotta, and R. W. Aldrich. 1990. Biophysical and molecular mechanisms of *Shaker* potassium channel inactivation. *Science.* 250:533–538.

Hoshi, T., W. N. Zagotta, and R. W. Aldrich. 1991. Two types of inactivation in *Shaker* K channels: effects of alterations in the carboxy-terminal region. *Neuron.* 7:547–556.

Isacoff, E. Y., Y. N. Jan, and L. Y. Jan. 1990. Evidence for the formation of heteromultimeric potassium channels in *Xenopus* oocytes. *Nature.* 345:530–534.

Iverson, L. E., and B. Rudy. 1990. The role of the divergent amino and carboxyl terminals domains on the inactivation properties of potassium channels derived from the *Shaker* gene of *Drosophila*. *J. Neurosci.* 10:2903–2916.

Kavanaugh, M. P., R. S. Hurst, J. Yakel, J. P. Varnum, J. P. Adelman, and R. A. North. 1992. Multiple subunits of a voltage dependent potassium channel contribute to the binding site for tetraethylammonium. *Neuron.* 8:493–497.

Khodorov, B., L. Shishkova, E. Peganov, and S. Revenko. 1976. Inhibition of sodium currents in frog Ranvier node treated with local anesthetics. Role of slow sodium inactivation. *Biochim. Biophys. Acta.* 433: 409–435.

Kirsch, G. E., J. A. Drewe, M. DeBiasi, H. A. Hartmann, and A. M. Brown. 1993. Functional interactions between K^+ pore residues located in different subunits. *J. Biol. Chem.* 19:13799–13804.

Kirsch, G. E., J. A. Drewe, H. A. Hartmann, M. Taglialatela, M. deBiasi, A. M. Brown, and R. H. Joho. 1992. Differences between the deep pores of K^+ channels determined by an interacting pair of nonpolar amino acids. *Neuron.* 8:499–505.

Kurz, L. L., R. D. Zuhlke, H. Zhang, and R. H. Joho. 1995. Side-chain accessibilities in the pore of a K^+ channel probed by sulfhydryl-specific reagents after cysteine-scanning mutagenesis. *Biophys. J.* 68:900–905.

Labarca, P., and R. MacKinnon. 1992. Permeant ions influence the rate of slow inactivation in Shaker K^+ channels. *Biophys. J.* A378.

Liman, E. R., J. Tytgat, and P. Hess. 1992. Subunit stoichiometry of a mammalian K+ channel determined by construction of multimeric cDNAs. *Neuron.* 9:861–871.

Lopez, G. A., Y. N. Jan, and L. Y. Jan. 1994. Evidence that the S6 segment of the Shaker voltage-gated K^+ channel comprises part of the pore. *Nature.* 367:179–182.

Lòpez-Barneo, J., T. Hoshi, S. H. Heinemann, and R. W. Aldrich. 1993. Effects of external cations and mutations in the pore region on C-type inactivation of *Shaker* potassium channels. *Receptors Channels.* 1:61–71.

Lu, Q., and C. Miller. 1995. Ag^{++} as a probe of pore forming residues in a K^+ channel. *Science.* 268:304–307.

MacKinnon, R. 1991. Determination of the subunit stoichiometry of a voltage-activated potassium channel. *Nature.* 350:232–235.

MacKinnon, R., R. W. Aldrich, and A. W. Lee. 1993. Functional stoichiometry of *Shaker* potassium channel inactivation. *Science.* 262:757–759.

McCormack, K., L. Lin, L. E. Iverson, M. A. Tanouye, and F. J. Sigworth. 1992. Tandem linkage of *Shaker* K channels subunits does not ensure the stoichiometry of expressed channels. *Biophys. J.* 63:1406–1411.

Narahashi, T. 1974. Chemicals as tools in the study of excitable membrane. *Physiol. Rev.* 54:813–889.

Ogielska, E. M., W. N. Zagotta, and R. W. Aldrich. 1994. The stoichiometry of C-type inactivation. *Biophys. J.* A282.

Panyi, G., Z. F. Sheng, L. W. Tu, and C. Deutch. 1995. C-type inactivation of a voltage gated K channel occurs by a cooperatve mechanism. *Biophys. J.* 69:896–903.

Tukey, J. W. 1977. Exploratory Data Analysis. Addison-Wesley Publishing, Reading, MA.

Yellen, G., D. Sodickson, T. Chen, and M. E. Jurman. 1994. An engineered cysteine in the external mouth of a K channel allows inactivation to be modulated by metal binding. *Biophys. J.* 66:1068–1075.

Zagotta, W. N., T. Hoshi, and R. W. Aldrich. 1989. Gating of single *Shaker* potassium channels in *Drosophila* muscle and in *Xenopus* oocytes injected with *Shaker* mRNA. *Proc. Natl. Acad. Sci. USA.* 86:7243–7247.

Zagotta, W. N., T. Hoshi, and R. W. Aldrich. 1990. Restoration of inactivation in mutants of *Shaker* potassium channels by a peptide derived from ShB. *Science.* 250:568–571.